Outstanding Superoxide Dismutase Catalytic Activity Of Simple Peptide-Based Nickel(II) Complexes

Pawel Guinard, Sarah Hostachy, Léa Diebold, Jacques Pécaut, Alan Le Goff, Carole Duboc, Pascale Delangle

How to cite: Angew. Chem. Int. Ed. 2024, e202409343
doi.org/10.1002/anie.202409343

Oxidative Stress Hot Paper

Outstanding Superoxide Dismutase Catalytic Activity Of Simple Peptide-Based Nickel(II) Complexes

Pawel Guinard, Sarah Hostachy, Léa Diebold, Jacques Pécaut, Alan Le Goff, Carole Duboc, and Pascale Delangle**

Abstract: We present here the most active synthetic Ni superoxide dismutase (NiSOD) mimic reported to date. Reactive oxygen species are aggressive compounds, which concentrations are tightly regulated in vivo. Among them, the superoxide anion, $O_2^{\bullet-}$, is controlled by superoxide dismutases. Capitalizing on the versatility of the Amino-Terminal Cu^{II}- and Ni^{II}-binding (ATCUN) peptide motif, we introduced positive charges around the Ni^{II} center to favor the interaction with the superoxide radical anion. At physiological pH, the pentapeptide H–Cys–His–Cys–Arg–Arg–NH_2 coordinates Ni^{II} after the deprotonation of one thiol, two amides, and either the second thiol or the N-terminal ammonium, leading to an equilibrium between the two N_3S_1 and N_2S_2 coordination modes. Under catalytic conditions, a k_{cat} value of $8.6(4)\times10^6$ $L.mol^{-1}.s^{-1}$ was measured. Within the first second, the catalyst remained undegraded with quantitative consumption of $O_2^{\bullet-}$ (completed up to 37 catalytic cycles). An extra arginine (Arg) was introduced at the peptide C-terminus to increase the global charge of the Ni^{II} complex from +1 to +2. This had no effect on the catalytic performance, highlighting the critical role of charge distribution in space as a determining factor influencing the reactivity.

Research in antioxidants is a dynamic and growing field, driven by their impact on human health and well-being since the uncontrolled concentration of reactive oxygen species (ROS) is associated with various chronic diseases and aging processes.[1] Additionally, their significance extends to the food industry, where they are used to preserve and stabilize food components. To design efficient antioxidants, one strategy focuses on mimicking natural enzymes.[2,3]

Among these, superoxide dismutases (SODs) emerge as highly efficient enzymes, finely tuned by evolution to catalytically dismutate the radical anion superoxide ($O_2^{\bullet-}$) with optimal performances. Featuring Cu/Zn, Fe, Mn, or Ni complexes at their active site, these redox metalloenzymes maintain cellular redox homeostasis by preventing oxidative stress, which results from the imbalance between ROS production and antioxidant defenses. Their impressive catalytic performance is attributed, in part, to common physicochemical parameters, including the redox potential of the active centers, finely tuned by the nature of the metal center and its first coordination sphere.[4] The second coordination sphere also plays a crucial role in facilitating interactions between the metal complex and $O_2^{\bullet-}$, as well as the reaction with protons.[2,4–6]

In the most recently discovered nickel superoxide dismutase (NiSOD),[7] the Ni^{II} ion displays a N_2S_2 square-planar geometry originating from the coordination of the terminal amine, an amido from the first peptide bond, and two thiolates from two cysteines (Scheme 1, left).[8] In the oxidized state, the Ni^{III} ion is further stabilized by the additional coordination of an imidazole of a histidine, resulting in a square-pyramidal geometry. The presence of thiolate donor ligands in the first coordination sphere of the Ni ion has intrigued chemists due to the known chemical sensitivity of such a sulfur-rich environment to reactive oxygen species, prompting the exploration of mimics. In the literature, two approaches have been pursued with the conception of either Ni-based metallopeptides, or low-molecular-weight synthetic Ni-based complexes.[9–11] The former typically demonstrate SOD-like activities in aqueous solutions (Scheme 1 and Table S1), while the latter, with a few exceptions,[12] lack catalytic activity but offer valuable insights into the mechanism or key structural features for optimal activities.[13–15]

In this context, we are developing an original strategy for designing NiSOD mimics based on the amino-terminal Cu^{II}- and Ni^{II}-binding (ATCUN) motif.[16] This scaffold was chosen for its ability to impose a square-planar geometry around the metallic ion, the stability it confers to the corresponding Ni^{II} complexes at physiological pH, and its versatility, which enables modulation of the metal coordination sphere.[17] In this study, we explored two mononuclear Ni^{II} complexes with optimized ATCUN-like peptide ligands, demonstrating exceptional SOD-like catalytic properties at physiological pH, and surpassing the performance of the

[*] Dr. P. Guinard, Dr. S. Hostachy, L. Diebold, Dr. J. Pécaut, Dr. P. Delangle
Univ. Grenoble Alpes, CEA, CNRS, Grenoble INP, IRIG, SyMMES, 38000 Grenoble, France
E-mail: pascale.delangle@cea.fr
Dr. P. Guinard, Dr. A. Le Goff, Dr. C. Duboc
Univ. Grenoble Alpes, CNRS, DCM, 38000 Grenoble, France
E-mail: carole.duboc@univ-grenoble-alpes.fr

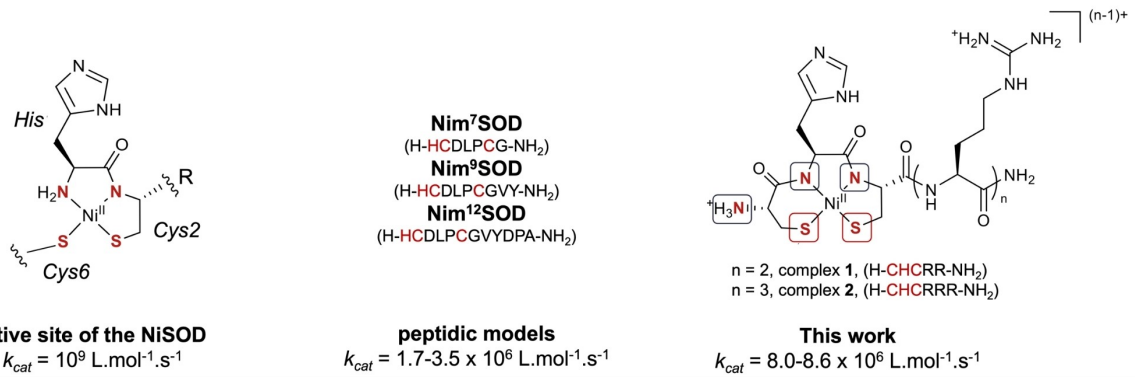

Scheme 1. Left: structure of the active site of NiSOD.[8] Middle: peptidic models developped from the 7th, 9th and 12th first amino-acids[9,18,19] of the N-terminus extremity of the protein (the sequence is indicated in brackets, with coordinating amino-acids enlightened in red), k_{cat} values were measured in catalytic conditions.[20] Right: structures of the major form of complexes **1** and **2** studied in this work, with their corresponding peptide sequences in brackets.

best-reported NiSOD mimics to date. (Scheme 1 and Table S1).

The design of the ATCUN-like peptide ligands was guided by previous evidence that the SOD-like activity can be enhanced with a histidine as the second amino acid to stabilize the oxidized Ni^{III} state and a cysteine in the N-terminal position that enables an equilibrium between a N_2S_2 and a N_3S_1 coordination mode (Scheme 1, right and Figure 1.B.).[16,21] Drawing inspiration from the SODs, we also integrated positively charged amino acids at the C-terminus, which are proposed to efficiently direct the $O_2^{\bullet-}$ substrate toward the catalytic center.[4,8,22–24] The guanidine side-chain of arginine was selected to introduce a positive charge due to its capacity to protonate in a guanidinium group at physiological pH and its inability to coordinate metal ions.

The ligand H–Cys–His–Cys–Arg–Arg–NH_2 was synthesized by standard solid-phase peptide synthesis with a C-terminal amide after cleavage, followed by purification using preparative reverse-phase HPLC. Complex **1** was then obtained by reacting the peptide and $NiSO_4$ in HEPES buffer (20 mM, [NaCl] = 0.1 M, pH 7.4). The complexation process appeared quite slow (*ca* 5 h for stabilization) as demonstrated by using UV/Visible spectroscopy, measuring the intensity of the LMCT band at 260 nm (Figure S1). This intense band ($\varepsilon = 17.0\times10^3$ L.mol^{-1}.cm^{-1}) was assigned to S–Ni and N–Ni transitions.[25] The ligand titration by Ni led to a linear increase in intensity up to one equivalent of Ni^{II}, which aligns with the quantitative formation of a complex with a 1:1 Ni:ligand stoichiometry (Figure S2). The presence of a d–d transition at 430 nm ($\varepsilon = 2.2\times10^2$ L.mol^{-1}.cm^{-1}) supports a square planar geometry around the Ni^{II} ion.[26] Beyond one equivalent of Ni^{II} and up to 1.5 equivalents, an absorption band at 400 nm appears, indicating the formation of polymetallic species. The monocationic complex **1** was detected as the major species in the (+)ESI-MS spectrum at m/z = 365.3, with no polymetallic species detected in sub-stoichiometric conditions (Figure S3). To prevent the presence of polymetallic complexes in solution, and to form the well-defined monometallic complex **1** only, the following experiments were performed with a Ni:ligand ratio of 0.9:1.

To ensure the complete formation of the complex at physiological pH, the effect of pH on Ni^{II} complexation was examined by UV–visible spectroscopy. The pH of aqueous solutions of complex **1** (45 μM) was adjusted using HCl or KOH. Spectra were recorded after stabilization in different batch samples for each pH. As illustrated in Figure 1.A, complex **1** is totally formed for a pH larger than 6, demonstrating quantitative Ni^{II} complexation at pH 7.4.

^{1}H NMR spectra of complex **1** revealed the presence of two distinct species in a 75:25 ratio, equilibrating at the NMR timescale. Two coordination modes were indeed systematically observed with Ni complexes derived from ATCUN-like peptides displaying a N-terminal cysteine.[27] The N_2S_2 species involves two thiolates and two amido groups in the Ni^{II} coordination, whereas the N_3S_1 species involves the N-terminal amine, one thiolate, and two amido groups (Figure 1.B). The NOESY spectrum evidences the dynamic exchange between these two coordination modes at the ^{1}H NMR time scale. This exchange is due to the rotation around the C(O)–Cα bond of Cys1 that allows Ni^{II} coordination either through the thiolate or the amino function of this residue (Figure 1D). The assignment of the proton NMR signals shows that the amino acids involved in the metal coordination, i.e. only the three first residues, exhibit significantly different chemical shifts for the two forms with the major species identified as the N_2S_2 coordination (75 %) (Figure 1.C). The proton signals of the arginine side chains display a single signature for Arg4 and Arg5, which is consistent with the lack of structure of the peptide C-terminus, which is less affected by the Ni^{II} ion coordination (Figures 1.C and 1.D).

The redox properties of complex **1** were investigated by cyclic voltammetry (CV) in HEPES buffer at physiological pH (20 mM, pH 7.4, [NaCl] = 0.1 M). Two irreversible oxidation processes corresponding to the monoelectronic Ni^{II}/Ni^{III} oxidation occur at E_{pc} of 0.33 and 0.57 V vs. SCE (Figure 1.E, red and grey, respectively). These redox events

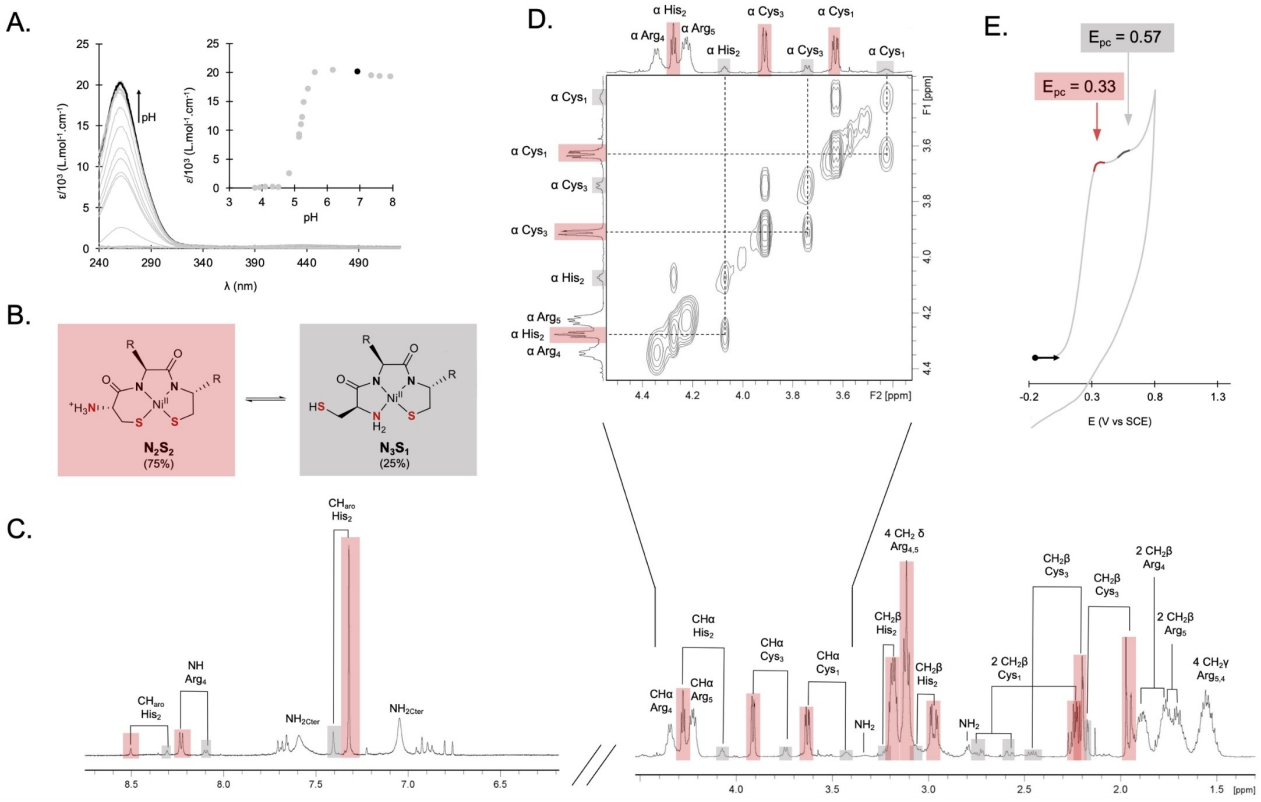

Figure 1. **A**. UV/Vis spectra of CHCRR (50 μM) with 0.9 equivalent of $NiSO_4$ in water as a function of pH. Bold: spectrum at pH 7. Inset: absorbance evolution at 260 nm as a function of pH. **B**. Structures of the two coordination modes of the studied complexes. **C**. 500 MHz ^{1}H NMR spectrum of CHCRR with 0.9 equivalent of Ni (complex **1**, 1.1 mM) at pH 7.35 in H_2O/D_2O (v/v: 90/10) at 298 K. The pH was adjusted by adding KOH. The spectrum between 1.5 and 5 ppm was acquired with water presaturation and the spectrum between 7 and 8.5 ppm with a watergate pulse sequence. Brackets connect the signals arising from the same protons in the N_2S_2 (red) and N_3S_1 (grey) coordination modes. **D**. Zoom on the α-proton region of the NOESY spectrum of **1**. Dashed lines highlight the exchange correlations between the N_2S_2 (red) and N_3S_1 (grey) coordination modes. **E**. CV of a solution of **1** (400 μM) in HEPES buffer (20 mM, [NaCl] = 0.1 M, pH 7.4). Working electrode: glassy carbon electrode. Reference electrode: SCE. Scan rate: 50 mV s^{-1}.

are associated with the two coordination modes of complex **1** in solution. As previously demonstrated for other Ni^{II} complexes,[16] the first irreversible system at E_{pc} 0.33 V corresponds to the more favorable N_2S_2 coordination mode. The shoulder at E_{pc} 0.57 V is attributed to the minor contribution of the N_3S_1 coordination mode in solution. Interestingly, the potentials of Ni^{II}/Ni^{III} redox systems of **1**, although higher than the one reported for the native NiSOD (0.05 V vs SCE),[5] are between the oxidation and reduction potentials of the superoxide radical anion (−0.42 and 0.67 V vs SCE,[4] respectively), suggesting a suitable range for catalytic SOD activity.

The catalytic SOD activity of **1** was assessed by stopped-flow experiments. Solutions of freshly prepared KO_2 in dimethyl sulfoxide (DMSO) with known $O_2^{\bullet-}$ concentrations (ε = 2686 L.mol^{-1}.cm^{-1}) were mixed with aqueous solutions of **1** at different concentrations. Under catalytic conditions, a significant increase in the rate of the $O_2^{\bullet-}$ disappearance is observed upon the addition of **1** evidencing SOD-like catalytic activity of **1** (Figure 2). The pseudo-first-order reaction rates (k_{obs}) linearly increase with the complex

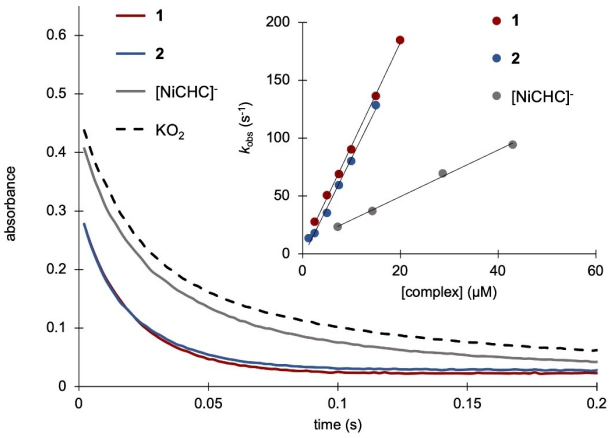

Figure 2. $O_2^{\bullet-}$ consumption followed by UV/Vis at 250 nm (ε = 2686 L.mol^{-1}.cm^{-1}) in the presence of 5 μM of each complex as a function of time. Inset: Linear regression (k_{obs} = f([complex]) with the slope corresponding to the k_{cat} value.

concentration. The resulting linear regression yields a k_{cat} value of $8.6(4)\times10^6$ L.mol^{-1}.s^{-1} (Figure 2, Inset). Since superoxide and hydrogen peroxide are known to oxidize thiols, we evaluated the stability of **1** by monitoring the intensity of the LMCT during the first second of the reaction when using a [$O_2^{\bullet-}$]/[**1**] ratio of 74. Within this short duration, no catalyst degradation is observed and $O_2^{\bullet-}$ is quantitatively consumed, indicating that under these conditions, **1** completes 37 catalytic cycles.

The k_{cat} value measured with **1** is significantly higher than the k_{cat} values reported in similar conditions for the Ni^{II} metallopeptides derived from the 7, 9, or 12 first amino acids of the native enzyme (1.7, 3.5, and 2.5×10^6 L.mol^{-1}.s^{-1}, respectively),[9,18,19] known to be the most efficient NiSOD mimics up to now. The performance of **1** also approaches 1% of the NiSOD efficiency ($\sim10^9$ L.mol^{-1}.s^{-1}).[28] With respect to the previously reported Ni^{II} complex derived from H-Cys-His-Cys-NH_2 (CHC) which is negatively charged,[16] the four-fold increase in the k_{cat} value ($2.0(1)\times10^6$ L.mol^{-1}.s^{-1} for [NiCHC]$^-$) highlights the remarkable impact of positive charges close to the metal center with introducing guanidinium functions (Table S1).

To further explore the impact of positive charges on SOD activity, a ligand with an extra arginine at its C-terminus was designed, H-Cys-His-Cys-Arg-Arg-Arg-NH_2 (CHCRRR). This modification results in a global +2 charge in the corresponding Ni^{II} complex, denoted **2**, while complex **1** has a global charge of +1 (Scheme 1, right). The synthesis, purification, and characterization of complex **2** followed the same procedure used for complex **1**. The UV/Vis spectra detected upon the formation of complex **2** are similar to that observed for complex **1**, with a d-d transition at 430 nm (1.5×10^2 L.mol^{-1}.cm^{-1}), and a LMCT feature at 260 nm (16.5×10^3 L.mol^{-1}.cm^{-1}) (Figure S4). A peak at m/z 443.5 in the (+) ESI-MS spectrum corresponding to [Ni+CHCRRR]$^{2+}$ is observed (Figure S5). As for **1**, all other experiments were conducted with a slightly sub-stoichiometric amount of Ni (0.9 equivalent) to prevent the formation of polymetallic species. The pH behavior on the formation of **2** is similar to that of **1**, with the quantitative formation of **2** at pH above 6.5 (Figure S6). A k_{cat} of $8.0(8)\times10^6$ L.mol^{-1}.s^{-1} was measured under catalytic conditions. As complex **1**, **2** is stable within the catalysis time and can complete 43 catalytic cycles when using a [$O_2^{\bullet-}$]/[**2**] ratio of 86.

The k_{cat} values measured for the SOD-like catalysts **1** and **2** are comparable, indicating that the additional arginine in **2** is too distant from the metal center to impact the interaction between $O_2^{\bullet-}$ and the catalytic site.

In all SODs, positively charged amino acids, such as lysines, are strategically positioned within the three-dimensional structure to create an electrostatic field that guides the substrate, i.e. the superoxide anion, towards the metal catalytic center.[8] Extensive investigations on MnSOD mimics have also emphasized the pivotal role of spatial charge distribution for SOD activity.[29–32] For instance, Policar et al. demonstrated that the introduction of positive charges in a series of MnSOD mimics enhanced SOD activity only if they were very close to the metal center (Table S1, Scheme 1),[32] highlighting the challenge of modelling long-range electrostatic effects in small molecular compounds. Optimizing the charge in NiSOD mimics is even more challenging due to the negative charge at the NiSOD catalytic site. In this study, appending arginine residues to small ATCUN motifs yielded Ni^{II} peptide complexes exhibiting catalytic activities comparable to, or even surpassing, those of positively charged MnSOD mimics (k_{cat} from 2.9 to 6.2×10^6 L.mol^{-1}.s^{-1}, see Table S1). However, further extending the polyarginine chain in complex **2**, which carries a 2+ charge, is unlikely to enhance SOD activity further, as previously observed with MnSOD mimics. Although the Ni^{II} complexes derived from an ATCUN-like scaffold described herein differ significantly from the enzyme active site, they are more efficient than peptide models derived strictly from the N-terminus of the protein. The highly preorganized ATCUN motif, with amidates and thiolates in a square-planar, rigid environment around the Ni^{II} cation, along with a positively charged arginine tail capable of attracting superoxide, represents a significant advancement in mimetic design.

In conclusion, through the rational design of NiSOD mimics, we engineered catalysts with SOD-like activity at physiological pH, exhibiting high performance and robustness. Leveraging the versatility of the ATCUN platform, we tailored the peptide chain for optimal catalytic properties. This work paves the way for future refinement and optimization, emphasizing the peculiar importance of the three-dimensional position of the charges. Continued efforts in this area are expected to yield compelling catalysts with diverse applications, ranging from basic research to therapeutic applications relevant to oxidative stress-related diseases.

Supporting Information

The authors have cited additional references within the Supporting Information.[16,20,32,33]

Acknowledgements

The authors gratefully acknowledge the research support of this work by the French National Agency for Research in the framework of the "Investissements d'avenir" Program (ANR-15-IDEX-02), the Labex ARCANE (ANR-11-LABX-003), and the CBH-EUR-GS(ANR-17-EURE-0003). The authors thank Pierre-Alain Bayle and Dr Ricardo Garcia for their support in the acquisition of the NMR spectra and of the stopped-flow data, respectively.

Conflict of Interest

The authors declare no conflict of interest.

Data Availability Statement

The data that support the findings of this study are available from the corresponding author upon reasonable request.

Keywords: Ni peptide-based complexes · NiSOD · ATCUN · SOD activity · oxidative stress

[1] C. C. Winterbourn, *Nat. Chem. Biol.* **2008**, *4*, 278–286.
[2] C. Policar, J. Bouvet, H. C. Bertrand, N. Delsuc, *Curr. Opin. Chem. Biol.* **2022**, *67*, 102109.
[3] D. P. Riley, *Chem. Rev.* **1999**, *99*, 2573–2588.
[4] C. Policar, in *Redox-Act. Ther.* (Eds.: I. Batinić-Haberle, J. S. Rebouças, I. Spasojević), Springer International Publishing, Cham **2016**, pp. 125–164.
[5] R. W. Herbst, A. Guce, P. A. Bryngelson, K. A. Higgins, K. C. Ryan, D. E. Cabelli, S. C. Garman, M. J. Maroney, *Biochemistry* **2009**, *48*, 3354–3369.
[6] V. V. Smirnov, J. P. Roth, *J. Am. Chem. Soc.* **2006**, *128*, 16424–16425.
[7] H. D. Youn, E. J. Kim, J. H. Roe, Y. C. Hah, S. O. Kang, *Biochem. J.* **1996**, *318(Pt 3)*, 889–896.
[8] D. P. Barondeau, C. J. Kassmann, C. K. Bruns, J. A. Tainer, E. D. Getzoff, *Biochemistry* **2004**, *43*, 8038–8047.
[9] M. Schmidt, S. Zahn, M. Carella, O. Ohlenschläger, M. Görlach, E. Kothe, J. Weston, *ChemBioChem* **2008**, *9*, 2135–2146.
[10] J. Shearer, K. L. Peck, J. C. Schmitt, K. P. Neupane, *J. Am. Chem. Soc.* **2014**, *136*, 16009–16022.
[11] E. P. Broering, P. T. Truong, E. M. Gale, T. C. Harrop, *Biochemistry* **2013**, *52*, 4–18.
[12] J. Domergue, J. Pécaut, O. Proux, C. Lebrun, C. Gateau, A. Le Goff, P. Maldivi, C. Duboc, P. Delangle, *Inorg. Chem.* **2019**, *58*, 12775–12785.
[13] D. Nakane, Y. Wasada-Tsutsui, Y. Funahashi, T. Hatanaka, T. Ozawa, H. Masuda, *Inorg. Chem.* **2014**, *53*, 6512–6523.
[14] E. M. Gale, A. C. Simmonett, J. Telser, H. F. Schaefer, T. C. Harrop, *Inorg. Chem.* **2011**, *50*, 9216–9218.
[15] P. T. Truong, E. M. Gale, S. P. Dzul, T. L. Stemmler, T. C. Harrop, *Inorg. Chem.* **2017**, *56*, 7761–7780.
[16] J. Domergue, P. Guinard, M. Douillard, J. Pécaut, S. Hostachy, O. Proux, C. Lebrun, A. Le Goff, P. Maldivi, C. Duboc, P. Delangle, *Inorg. Chem.* **2023**, *62*, 8747–8760.
[17] P. Gonzalez, K. Bossak, E. Stefaniak, C. Hureau, L. Raibaut, W. Bal, P. Faller, *Chem. Eur. J.* **2018**, *24*, 8029–8041.
[18] K. P. Neupane, J. Shearer, *Inorg. Chem.* **2006**, *45*, 10552–10566.
[19] J. Shearer, L. M. Long, *Inorg. Chem.* **2006**, *45*, 2358–2360.
[20] D. Tietze, J. Sartorius, B. Koley Seth, K. Herr, P. Heimer, D. Imhof, D. Mollenhauer, G. Buntkowsky, *Sci. Rep.* **2017**, *7*, 17194.
[21] J. Domergue, P. Guinard, M. Douillard, J. Pécaut, O. Proux, C. Lebrun, A. Le Goff, P. Maldivi, P. Delangle, C. Duboc, *Inorg. Chem.* **2021**, *60*, 12772–12780.
[22] E. D. Getzoff, D. E. Cabelli, C. L. Fisher, H. E. Parge, M. S. Viezzoli, L. Banci, R. A. Hallewell, *Nature* **1992**, *358*, 347–351.
[23] E. D. Getzoff, J. A. Tainer, P. K. Weiner, P. A. Kollman, J. S. Richardson, D. C. Richardson, *Nature* **1983**, *306*, 287–290.
[24] S. Folcarelli, A. Battistoni, M. Falconi, P. O'Neill, G. Rotilio, A. Desideri, *Biochem. Biophys. Res. Commun.* **1998**, *244*, 908–911.
[25] R. T. Stibrany, S. Fox, P. K. Bharadwaj, H. J. Schugar, J. A. Potenza, *Inorg. Chem.* **2005**, *44*, 8234–8242.
[26] H. Kozlowski, B. D.-L. Révérend, D. Ficheux, C. Loucheux, I. Sovago, *J. Inorg. Biochem.* **1987**, *29*, 187–197.
[27] J. D. Van Horn, G. Bulaj, D. P. Goldenberg, C. J. Burrows, *JBIC J. Biol. Inorg. Chem.* **2003**, *8*, 601–610.
[28] P. A. Bryngelson, S. E. Arobo, J. L. Pinkham, D. E. Cabelli, M. J. Maroney, *J. Am. Chem. Soc.* **2004**, *126*, 460–461.
[29] I. Batinic-Haberle, L. Benov, I. Spasojevic, I. Fridovich, *J. Biol. Chem.* **1998**, *273*, 24521–24528.
[30] I. Spasojević, I. Batinić-Haberle, J. S. Rebouças, Y. M. Idemori, I. Fridovich, *J. Biol. Chem.* **2003**, *278*, 6831–6837.
[31] J. S. Rebouças, I. Spasojević, D. H. Tjahjono, A. Richaud, F. Méndez, L. Benov, I. Batinić-Haberle, *Dalton Trans.* **2008**, 1233.
[32] H. Y. V. Ching, I. Kenkel, N. Delsuc, E. Mathieu, I. Ivanović-Burmazović, C. Policar, *J. Inorg. Biochem.* **2016**, *160*, 172–179.
[33] G. L. Ellman, *Arch. Biochem. Biophys.* **1959**, *82*, 70–77.

Manuscript received: May 17, 2024
Accepted manuscript online: July 16, 2024
Version of record online: ■■, ■■

Communication

Oxidative Stress

P. Guinard, S. Hostachy, L. Diebold, J. Pécaut, A. Le Goff, C. Duboc,* P. Delangle* **e202409343**

Outstanding Superoxide Dismutase Catalytic Activity Of Simple Peptide-Based Nickel(II) Complexes

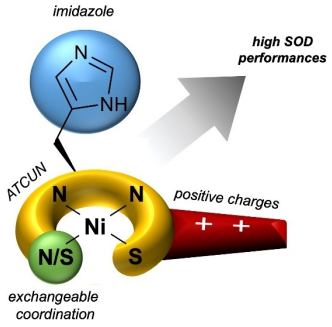

Be positive! A novel Ni superoxide dismutase mimic was engineered, taking advantage of the versatility of the Amino Terminal Cu^{II}- and Ni^{II}-binding (ATCUN) motif to introduce positive charges around the Ni^{II} center. This strategy yielded the most potent synthetic Ni-SOD mimic reported to date, in terms of catalytic efficacy and stability.